

## Reconstruction of atmospheric neutrino events in JUNO

**Marta Colomer Molla,<sup>a,\*</sup> Mariam Rifai,<sup>b,c</sup> and Rosmarie Wirth<sup>d</sup> on behalf of the JUNO collaboration**

<sup>a</sup>*Inter-university Institute for High Energies, Université libre de Bruxelles (ULB), Brussels, Belgium*

<sup>b</sup>*Forschungszentrum Jülich GmbH, Nuclear Physics Institute IKP-2, Jülich, Germany*

<sup>c</sup>*III. Physikalisches Institut B, RWTH Aachen University, Aachen, Germany*

<sup>d</sup>*Institute of Experimental Physics, University of Hamburg, Hamburg, Germany*

*E-mail: [rosmarie.wirth@desy.de](mailto:rosmarie.wirth@desy.de), [m.rifai@fz-juelich.de](mailto:m.rifai@fz-juelich.de), [marta.colomer@ulb.be](mailto:marta.colomer@ulb.be)*

The Jiangmen Underground Neutrino Observatory (JUNO) is a 20 kton multipurpose liquid-scintillator detector whose main goal is the determination of the neutrino mass ordering using the measurement of the vacuum dominated oscillation pattern of reactor anti-neutrinos from eight reactor cores. The sensitivity of JUNO to the neutrino mass ordering can be enhanced via a combined analysis of reactor anti-neutrinos with atmospheric neutrinos, in which the matter-dominated oscillation depends on the mass ordering. Such an analysis requires a precise reconstruction of the energy and the direction of atmospheric neutrinos. As the largest liquid-scintillator detector ever built, JUNO will also be able to measure the atmospheric neutrino flux down to lower energies than the current large Cherenkov detectors. This poster presents the reconstruction of the energy of atmospheric neutrinos with a machine learning approach and the direction reconstruction with a novel approach. While the machine learning approach relies on the geometrical representation of the detector with a Graph Convolutional Neural Network, the latter focuses on the reconstruction of the photon emission topology in the JUNO detector. The results presented are based on Monte-Carlo simulations, including for the first time the full electronics response, calibration and waveform reconstruction.

38th International Cosmic Ray Conference (ICRC2023)  
26 July - 3 August, 2023  
Nagoya, Japan



---

\*Speaker

## 1. Introduction

The Jiangmen Underground Neutrino Observatory (JUNO), with its large liquid scintillator (LS) volume and located 700 m underground, will be able to detect atmospheric neutrinos, among other natural neutrino sources. The main goal of JUNO is to determine the neutrino mass ordering (NMO) at  $3\sigma$  level within  $\sim 6$  years of data taking by observing reactor neutrinos from two nuclear power plants at  $\sim 53$  km distance. The JUNO detector design and physics goals are discussed in details in [1]. Here, we focus on the atmospheric neutrino analysis at GeV energies. In fact, the cosmic muon background in JUNO can be tagged thanks to two veto detectors: a water pool surrounding the central detector which will act as a cherenkov detector, and a top tracker composed of three plastic scintillator layers. The synergies with reactor neutrino vacuum oscillations can therefore be exploited to boost JUNO's sensitivity to the NMO. Indeed, the atmospheric neutrino oscillation pattern is sensitive to matter effects, which depend on the neutrino mass ordering. For that, one needs to consider that matter effects on neutrino oscillations depend on the neutrino energy and zenith angle, and the oscillation probabilities change as well with the neutrino flavor. The reconstruction of GeV events in large unsegmented LS detectors like JUNO is not an easy task (large energy deposit lightening the full detector at a time, event tracks not fully contained in the detector, etc.). Here, we propose two different approaches to reconstruct the event topology, giving access to the direction of the primary lepton, and the neutrino energy, that will be used in a final oscillation analysis.

## 2. Data

For this work, Monte Carlo (MC) data produced with the GENIE [3] generator V3.00.06 and the latest version of the official JUNO software [2] has been used. The 17612 large photomultipliers (LPMTs) of JUNO are considered here. Compared to the work in [7], which used an older GEANT4 detector simulation and MC truth information, the data used for the results that will be shown here include: a new PMT and LS models (see [8]), the simulation of all possible reflections (internal, with steel structure, etc.), as well as the electronics effects.

## 3. Topological Track Reconstruction

The approach of this reconstruction method consists on obtaining the spatial probability distribution for the origin of the photon emission. The algorithm is described in detail in [4–6]. The method relies on a model (probability distribution functions, PDFs) describing the direct photon propagation time and the charge detected as a function of the distance and angle with respect to the PMTs detecting the photon (see Fig. 1 for an illustration). The procedure to build these PDFs was described in [7]. The analytical PDFs are shown in figure 2. The PDFs include the attenuation length and absorption of the liquid scintillator, the PMT angular acceptance, and internal reflections.

The updates of this work with respect to the previous preliminary results are the following: i) using as input data the first hit time and total charge observed by each PMT instead of the full PMT waveform, and ii) incorporating the effect of the waveform reconstruction to extract the reconstructed first hit time (FHT) and charge detected by each PMT. In fact, it was shown in [9] that when dealing with GeV events (up to millions of photoelectrons deposited in the detector), the

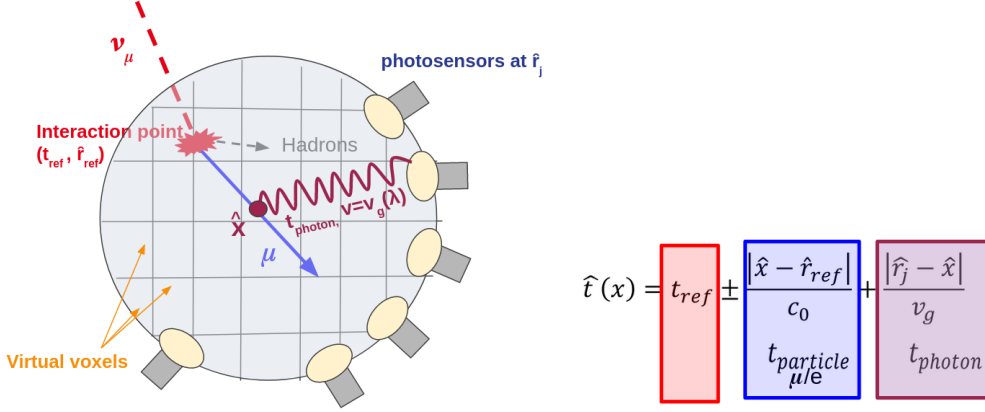


**Figure 1:** Illustration of the basic information on photon propagation used for the topological reconstruction. A neutrino event interacts with the LS of the JUNO central detector at the reference point  $r_{ref}$  at the reference time  $t_{ref}$ . The primary charged lepton product of the interaction travels along a straight track through  $x$ . The charged lepton may be accompanied by secondary hadronic emission, depending on the interaction channel. A photon emitted with wavelength  $\lambda$  at a point  $x$  reaches the photosensor at distance  $r_j$  with a speed equal to the wavelength-dependent group velocity  $v_g(\lambda)$ .

information on the first hit detected by each PMT is enough to reconstruct the direction of GeV particles in JUNO, while allows to reduce the requirements for data storage and the computational time of the algorithm, without degrading the reconstruction performance.

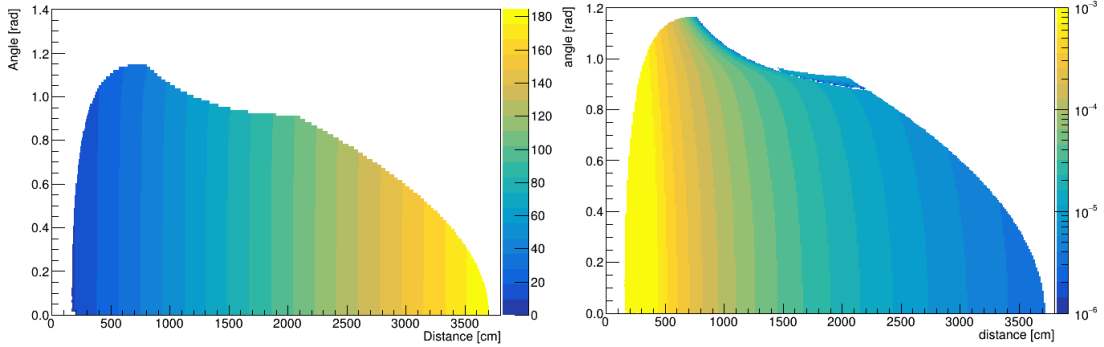


**Figure 2:** Time (left) and charge (right) PDFs, and a function of the distance and angle (X and Y-Axis). The Z-axis shows mean time propagation time of photons in the LS from the emission point to the PMT observing the light for the time PDF, and the fraction of the total charge deposited observed by each PMT for the charge PDF.

### 3.1 Time correction to use the reconstructed FHT after calibration

The topological reconstruction method relies on a local reference point in space and time. In the previous preliminary work, the true MC interaction time and vertex were used for each event. When one moves to the full simulation including electronics (trigger), calibration and waveform reconstruction, the hit time distribution and thus the first hit time reconstruction, are shifted with respect to the true reference time, used to build the PDFs. This is shown in Fig. 3 (left).

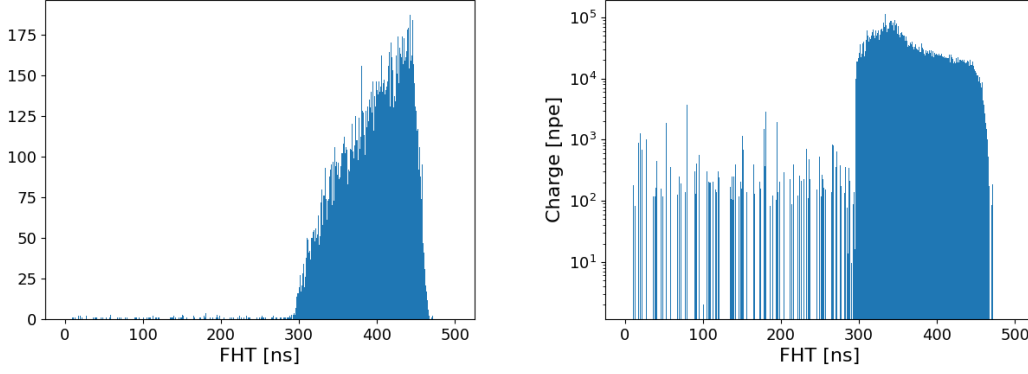


**Figure 3:** Left figure: distribution of the first hit time over all LPMTs in JUNO for a simulated atmospheric neutrino event. Right figure: FHT distribution weighted by the total charge in the PMT.

The idea is to find the time  $T_0$  in the distribution of the FHT weighted with the charge (Fig. 3 right) which corresponds to the start of the physical signal first hit times, and correct the FHT values in data for it to match the reference time in the algorithm and PDFs. The way of doing so is to find the time bin (1ns width) for which the charge in the PMTs with FHT value within the next 20 ns significantly exceeds (at least three times greater) the average charge for PMTs with FHT below 200 ns, given the 300 ns pre-trigger time window in the electronic simulation. This ensures the rise of the distribution due to the signal start with respect to PMTs having low FHT value driven by noise hits. The total charge detected by each PMT is computed in the corresponding signal time window.

### 3.2 Results

In this sub-section, we show the reconstructed emission probability maps obtained for two atmospheric neutrino events as an example, both corresponding to the charged current interaction of a  $\sim 3$  GeV muon neutrino. The output of the reconstruction in Fig. 4 shows that the emission probability maps match well with the true particle track in red, with higher probability of the photons being emitted from where truly the particle was passing through. This allows to infer the event topology and the particle direction. Since the highest probability is reconstructed near the interaction point, an estimation of the vertex position can also be obtained.

## 4. Energy reconstruction with graph convolutional networks

The energy reconstruction is based on graph convolutional networks, feeding the geometrical detector representation as the graph into the network. This is achieved by assigning a node to each used PMT. These nodes are connected over edges to their spatially closest neighbors. This allows convolution on the detectors skin, without a loss of geometrical information.

To reconstruct the energy, all large PMTs of JUNO (17612) are considered. During training, each node gets the input features. The used inputs are the first hit time and the number of photoelectrons (npe) for each PMT, and the npe over time distribution summed over all LPMTs,  $\sum \text{npe}(t)$ . For the Graph Convolution an implementation after Kipf and Welling [10] is used.

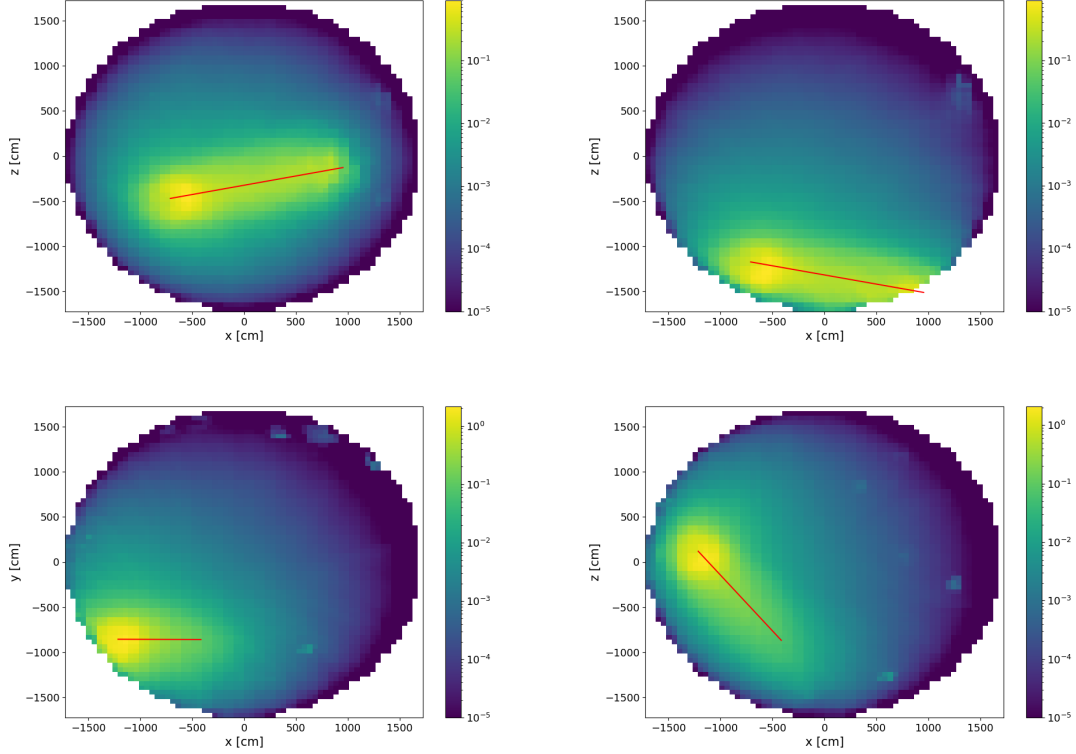


**Figure 4:** Reconstruction results after 6 iterations, projected over the  $z$  (right) and  $y$  (left) planes. On top, an atmospheric  $\nu_\mu$ -CC interaction where small hadronic contribution. The bottom shows an event where a significant part of the neutrino energy goes into secondary hadronic emission.

#### 4.1 Architecture

The network architecture consists of three parts: a Graph Convolution, a 1D Convolution, and a Fully Connected Network. The network architecture, described below, is shown schematically in Fig. 5. Each block can be used several times in a row with adjusted parameters to improve the reconstruction performance. The number of blocks, features and clusters are all hyper-parameter for this architecture, and they have been adjusted in a Bayesian optimization. The Mean-Squared-Error is used as loss function. On all layers, but the last one, the ReLU activation function is used.

For the Graph Convolution, an adapted form of the ResNet Architecture [11] is used. In these blocks, the amount of node features  $N_F$  needs to be constant. For this reconstruction, a Graph Convolution layer with increasing node features is followed by one or more ResNet blocks. The number of blocks and features are increasing in a pyramid scheme. After the ResNet blocks, a pooling method is implemented. Here, the Graph Partition Pooling [12] method is used. This method reduces the number of nodes in the graph by clustering the nodes using the k-means++ algorithm and pooling on maximal values on each cluster. This method is the first one published that suitable for this task: pooling a Graph that is used as a detector representation.

The input data for this Graph Convolution are the FHT and npe of each PMT. The 1D Convolution uses as input the charge (npe) over time distribution summer over all PMTs. In this part, 1D

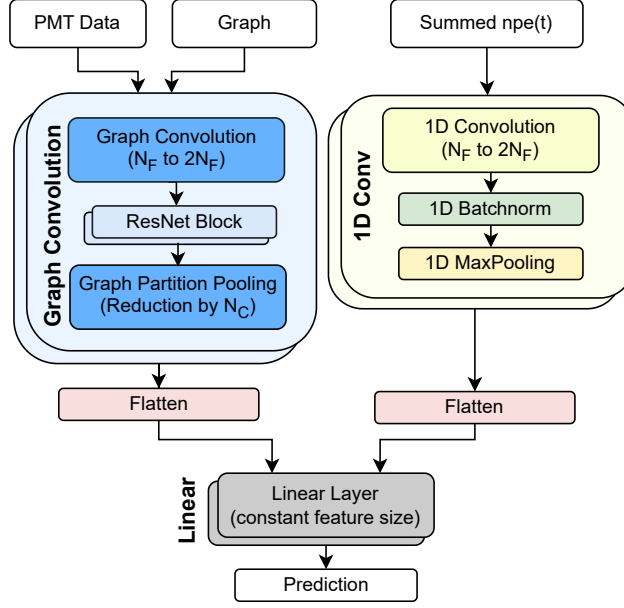


**Figure 5:** Schematics of used architecture,  $N_F$  is short for number of features used in the specific Layer,  $N_C$  the number of clusters used by Graph Partition Pooling to reduce the amount of nodes of the graph. For the Graph Convolution 2 input features are used for the 17612 nodes, one node represents one LPMT. The 1D Convolution takes the charge over time distribution as input, which has 100 bins. Both parts are combined in some linear layers, which return the prediction.

Convolution layers with increasing amount of features alternate with 1D MaxPooling. Afterwards, flattening is used to adjust the dimensions. At the end, both outputs are appended in one tensor, which is used as the input for the Fully Connected Network. At this step, the outputs are processed together and the amount of nodes is decreased to fit the prediction.

## 4.2 Results

The visible energy of atmospheric neutrino events is reconstructed with the previously described approach. To check the reconstruction performance, the true (in the following label) visible energy is compared with the visible energy predicted by the neural network described above. Compared to previous studies (see [7], the quenching effect has been include in the visible energy). The predicted visible energies are plotted against the label ones in figure 6. Figure 7 shows the differences between the label and predicted visible energy (in percentage), defined as:

$$dE [\%] = \frac{(E_{\text{label}} - E_{\text{prediction}})}{E_{\text{label}}} \cdot 100 \quad (1)$$

with  $E_{\text{label}}$  as label energy and predicted energy  $E_{\text{prediction}}$ .

The predicted values show a systematic offset towards lower predicted visible energies. The mean of the  $dE$  distribution is at 0.64%. To correct for this bias, the reconstructed energies are binned in range [0.5, 15] GeV with a bin width of 0.5 GeV. For each energy bin, the reconstructed energy is weighted by a correction factor. Those factors are multiplied with the predicted energies

in each bin, and the energy deviation is calculated for each correction factor. The energy deviations are fitted to the correction factors with a linear function. For each function, the factor for  $dE = 0$  is found and used as correction factor. In this way, each bin is corrected individually. The results shown in the following are bias corrected, with the described method. Fig. 6 and 7 show the bias corrected dependence of the label to predicted energy as a narrow linear distribution. One can see that the differences  $dE$  are well centered around  $dE = 0$  after bias correction. The resulting resolution is of  $\sim 2\%$ . For comparison, a simple linear regression approach between the detector charge npe and the true visible energy results in a resolution of around 5 %.

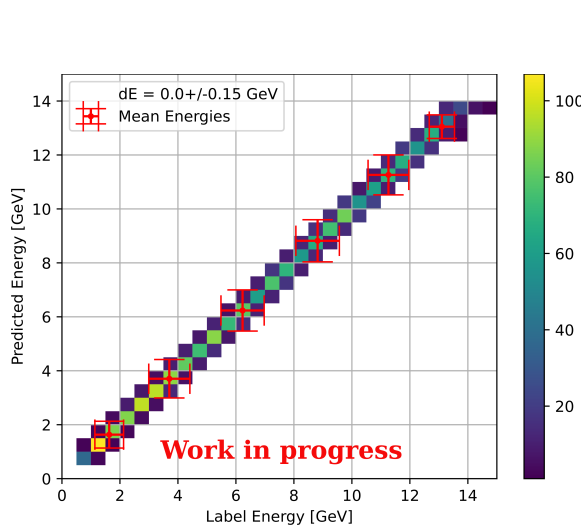


**Figure 6:** Predicted visible energy against label visible energy, after bias correction.

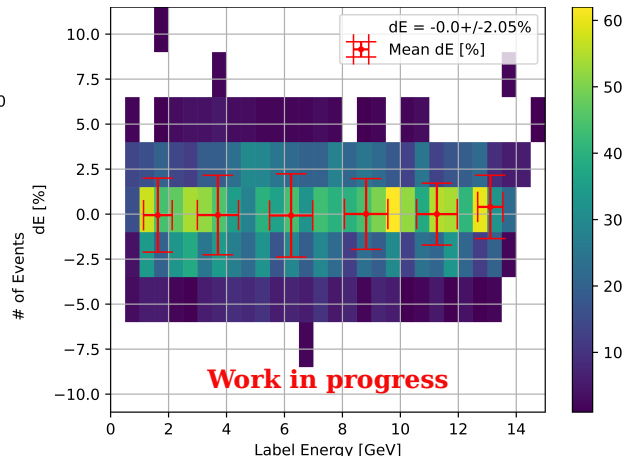


**Figure 7:** Difference between label and predicted visible energy in percentage, after bias correction. Overall mean and standard deviation are  $0.0 \pm 2.05\%$ .

## 5. Conclusions and outlook

This proceedings present two different approaches to reconstruct the energy and direction of GeV events in a liquid scintillator detector. We show the capability of JUNO to reconstruct atmospheric neutrinos within the requirements for oscillation studies. Next steps of this work will include an optimisation of the algorithms, their implementation into the official JUNO software, and the studies on the systematics related to different neutrino generators.

## References

- [1] A. Abusleme et al., *Progr. Part. Nucl. Phys.* 123 (2022) 103927
- [2] T. Lin et al., JUNO collaboration, "Parallelized JUNO simulation software based on SNIPEr", *J. of Physics: Conf. Series* 1085 (2018) 032048
- [3] C. Andreopoulos et al., *Nucl. Instrum. Meth. A* 614:87-104 (2010)
- [4] B. S Wonsak et al., *JINST* 13 (2018) 07, P07005
- [5] H. Rebber et al., *JINST* 16 (2021) 01, P01016
- [6] D.J. Meyhöfer, "3D Topological Reconstruction in JUNO applied to GeV events", PhD thesis (2020)

- [7] R. Wirth, M. Colomer, M. Rifai, "*Reconstruction of atmospheric neutrino events at JUNO*", PoS(ICHEP2022)1114 (2022)
- [8] A. Abusleme et al, JUNO collaboration, EPJC 82 (2022) 12, 1168
- [9] X. Liu, "A pure probabilistic approach to event reconstruction at JUNO", PoS(ICHEP2022)977
- [10] T.N. Kipf and M. Welling, "Semi-Supervised Classification with Graph Convolutional Networks", arXiv:1609.02907 (2016)
- [11] K. He et al., "Deep Residual Learning for Image Recognition", arXiv:1512.03385 (2015)
- [12] M. Bachlechner et al., "Partition Pooling for Convolutional Graph Network Applications in Particle Physics", arXiv:2208.05952